Journal of Chromatography A, 1218 (2011) 1995–2006

Contents lists available at ScienceDirect

Journal of Chromatography A

journal homepage: www.elsevier.com/locate/chroma

Effects of the gradient profile, sample volume and solvent on the separation in very fast gradients, with special attention to the second-dimension gradient in comprehensive two-dimensional liquid chromatography

Pavel Jandera*, Tomáš Hájek, Petr Česla

Department of Analytical Chemistry, University of Pardubice, Studentská 573, 53210 Pardubice, Czech Republic

ARTICLE INFO

Article history:
Available online 30 October 2010

Key words:
Two-dimensional comprehensive LC × LC
Fast gradients
Porous shell particles
Sample volume
Sample solvent
Bandwidths
Band distortion

ABSTRACT

Gradient elution provides significant improvement in peak capacity with respect to isocratic conditions and therefore should be used in comprehensive two-dimensional LC × LC, both in the first and in the second dimension, where, however, gradients are limited to a short time period available for separation, usually 1 min or less. Gradient conditions spanning over a broad mobile phase composition range in each second-dimension fraction analysis are used with generic "full in fraction" (FIF) gradients. "Segment in fraction" (SIF) gradients cover a limited gradient range adjusted independently to suit changing lipophilicity range of compounds transferred to the second dimension during the first-dimension gradient run and to provide regular coverage of the two-dimensional retention space. Optimization of the gradient profiles is important tool for achieving high two-dimensional peak capacity and savings of the separation time in comprehensive LC × LC. Calculations based on the well-established gradient-elution theory can be used to predict the elution times and bandwidths in fast gradients, taking into account increased probability of pre-gradient or post-gradient elution. The fraction volumes transferred into the second dimension may significantly affect the second-dimension bandwidths, especially at high elution strength of the fraction solvent, which may cause even band distortion or splitting in combined normal-phase (HILIC)–RP systems, but also in some two-dimensional RP–RP systems. In the present work, the effects of the fast gradient profile, of the sample volume and solvent on the elution time and bandwidths were investigated on a short column packed with fused-core porous-shell particles, providing narrow bandwidths and fast separations at moderate operating pressure.

1. Introduction

Gradient elution allows separations of samples containing compounds with largely different retention in a single run. It is well known that the maximum number of peaks that can be separated side-by side in a given experimental time, so-called peak capacity, n_c, is considerably higher in gradient chromatography than at isocratic conditions [1–4], due to narrower peaks; further the coverage of the retention space in a fixed time of separation is often more regular in comparison to the isocratic elution mode. Like in one-dimensional chromatography, gradient elution provides significant improvement in peak capacity in comprehensive two-dimensional LC × LC, hence, gradient elution should be preferred in on-line two-dimensional comprehensive liquid chromatography. For maximum increase in the two-dimensional peak capacity, second-dimension gradients should provide separation selectivity largely different from the first-dimension one [5,6] and the fraction transfer should not contribute significantly to band broadening [7], which is often not easy to achieve in practice.

The contribution of the second dimension is essential for the overall two-dimensional LC × LC separation performance [8]. Fast separation in the second dimension is crucial for successful 2D comprehensive LC × LC separations. Further, if the resolution obtained in the first dimension is not to be significantly impaired by sample re-mixing in the fractions prior to the injection onto the second-dimension column due to "undersampling", at least 3–4 fractions should be collected per the first-dimension peak width for the second-dimension separation (Murphy–Schure–Foley rule) [9]. Gradient elution provides approximately constant bandwidths of the early and of the late eluting peaks, hence approximately

* Corresponding author. Tel.: +420 466 037 023; fax: +420 466 037 068.
E-mail address: Pavel.Jandera@upce.cz (P. Jandera).

0021-9673/$ – see front matter © 2010 Elsevier B.V. All rights reserved.
doi:10.1016/j.chroma.2010.10.095

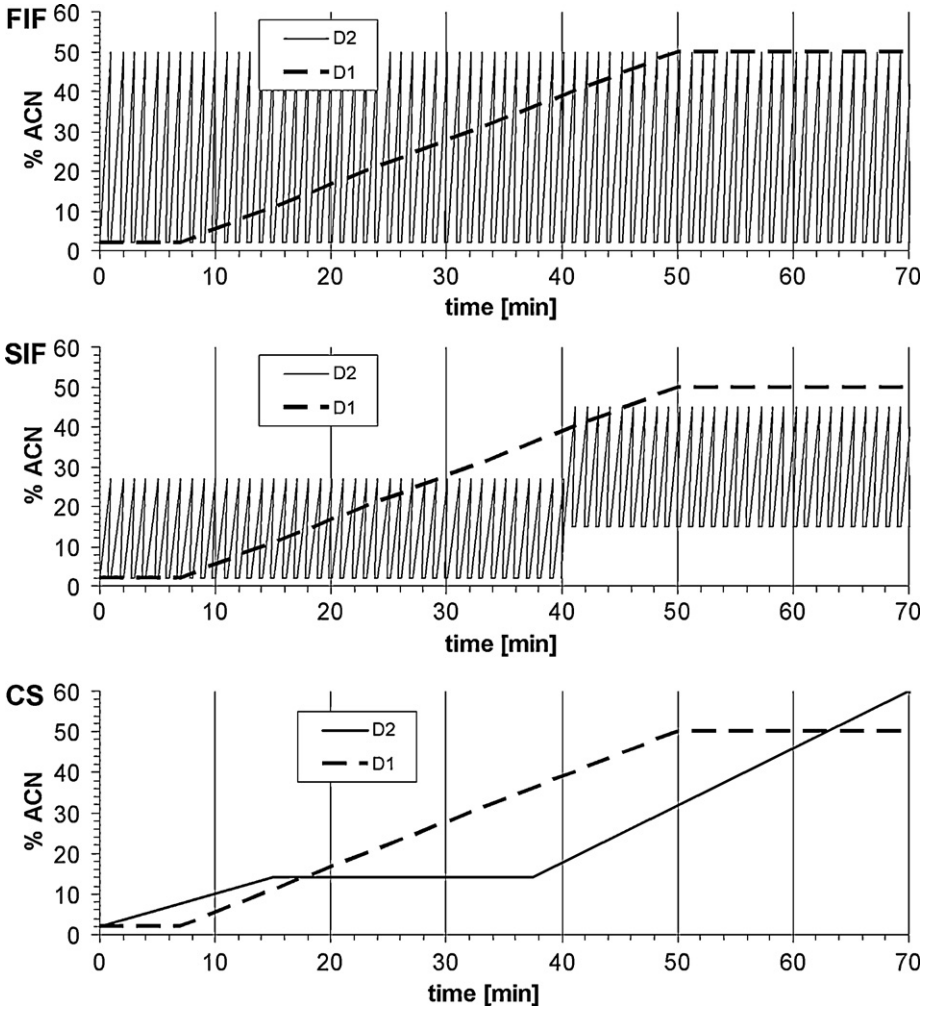

Fig. 1. Examples of second-dimension gradient profiles in comprehensive LC × LC. FIF, full in fraction second dimension gradient; SIF, segment in fraction second dimension gradient; CS, continuously shifting second dimension gradient.

equal number of fractions per a first-dimension peak during the whole gradient separation. This is a significant advantage to isocratic elution mode, where the bandwidths regularly increase with increasing elution times and the fraction number per peak regularly changes at a constant fraction cycle (modulation) time.

The second-dimension gradients are limited to a short time during a first-dimension fraction collection period. Using fast second dimension gradients (20–60 s, including the post-gradient column re-equilibration time), it was possible to accomplish on-line comprehensive LC × LC separations in 30–45 min [10–12]. Fast gradient separations within a fixed time improve at high linear flow velocities on short efficient columns, such as sub-2 μm columns at very high operation pressures. Similar results can be achieved at high flow rates allowed by the pressure limits with standard HPLC instrumentation (to 400 bar) using monolithic columns [13–15], or columns packed with fused-core porous-shell particles, which however usually provide better efficiencies at high flow rates [11,14,16].

To achieve high orthogonality and two-dimensional (2D) peak capacity, the gradient conditions should be carefully optimized, both in the first and in the second dimension. Gradients run simultaneously in the first and in the second dimension are mainly used in reversed-phase (RP) two-dimensional systems with different bonded stationary phase chemistry, or – less often – different mobile phase gradients [17], but can be applied also in normal phase (HILIC) LC × LC.

Second-dimension gradients can be classified as generic "Full in fraction" (FIF), "Segment in fraction" (SIF) and "Continuously shifting" (CS) gradients (Fig. 1) [18]. The first-dimension gradient profiles are represented as broken lines and for the second-dimension gradients as full lines. There may be important differences in the resolution, regularity of the coverage of the two-dimensional retention plane and of the overall separation time, so that the individual gradient types have characteristic advantages and disadvantages [18]:

1. Generic steep gradients with an equal mobile phase composition change in each second-dimension run – "full in fraction" (FIF) gradients – cover broad composition range between the initial and final mobile phases in a very short time and offer efficient bandwidth suppression. However post-gradient column re-equilibration should be included in the separation time of each second-dimension fraction separation, which significantly diminishes the peak capacity in the second dimension and may result in less regular coverage of the available retention space and even possible carry-over of strongly retained compounds to the next fraction.
2. "Segment in fraction" (SIF) second-dimension gradients employ different partial mobile phase composition changes in several subsequent time segments and combine some advantages of the FIF and CS gradient types. They are less steep than FIF gradients, but still provide significant bandwidth suppression; the sample

carry-over can be avoided by using several segments with various mobile phase composition ranges that can be adjusted to suit the retention (the lipophilicity range) of the sample compounds.
3. "Continuously shifting" (CS) gradients are useful especially in 2D systems with partly correlated retention, such as RP × RP. They are relatively shallow and usually provide larger bandwidths than FIF gradients, but enable faster second dimension separation, as post-gradient equilibration is not necessary within the individual cycles. The separation space is more regularly covered and sample carry-over can be avoided by adjusting parallel gradient profiles in the first and in the second dimension [19].

Even though the theory of gradient elution is well established [20–23], its validity has not been yet systematically studied with very steep gradients (1 min or less) run at high flow-rates (3–4 ml/min) on short columns (2–3 cm long), conditions which are necessary for fast second-dimension SIF or FIF gradient separations. With fast steep gradients, gradient pre-elution or post-gradient elution are more likely than with slower gradients and longer columns and should be avoided with second-dimension gradients, as it may reduce the peak capacity and even cause sample cross-over to the next fraction.

Recently, we presented an approach for calibration, prediction and optimization of gradient conditions for fast two-dimensional RP × RP separations of samples with broad lipophilicity distribution and applied this approach to comprehensive 2D separations of natural antioxidants with a DIOL or polyethylene glycol column in the first dimension and a porous-shell fused-core C18 column in the second dimension [18]. One objective of the present work was investigating the pre-elution and post-gradient elution of compounds with different lipophilicities controlling their retention in reversed-phase LC with fast steep gradients.

The sample solvent may very significantly affect the quality of separation [24–37]. It is well known that samples dissolved in a weaker solvent than the mobile phase (such as in water in reversed-phase LC) are adsorbed in a narrow zone at the top of the column, so that the bandwidths at the time of elution are suppressed with respect to the injected sample volume. This "on-column sample focusing" can be used to increase the detection selectivity by injecting relatively large volumes of diluted samples [35,36]. On the other hand, injection of a sample dissolved in a stronger eluent than the mobile phase may cause band broadening or even distortion or splitting [24–30], which was attributed to solubility effects [31], or to differences in the viscosity of the sample solvent and that of the mobile phase, giving rise to "viscous fingering", which can affect the dispersion of localized samples in porous media [25,32–34]. Some experimental results suggest that the differences in the elution strength of the sample solvent and the mobile phase are the most important factor affecting this undesirable behavior [25]. These effects may be particularly detrimental with short highly efficient columns used in the second dimension, which generate very small peak volumes [37].

In 2D LC × LC, fractions dissolved in the first-dimension mobile phase are usually transferred to the second dimension with different composition of the mobile phase. As a rule, a more retentive column and a stronger mobile phase should be used in the second dimension with respect to the first dimension in comprehensive LC × LC, to suppress the band broadening caused by non-matching elution strength in the two dimensions and to use the advantage of "sample focusing effect". In practice, this approach is rather difficult to apply, unless there is a strong correlation between the sample retention in the first and in the second dimension, which however impairs the system orthogonality and hence 2D peak capacity.

Poor mobile phase compatibility may negatively affect 2D reversed-phase gradient separations. However, the problem is much worse when a reversed-phase and a normal-phase (or HILIC) mode are coupled in an on-line comprehensive LC × LC system. Mobile phases rich in acetonitrile used in HILIC operation are strong eluents in reversed-phase systems, whereas mobile phases with relatively high concentrations of water used in reversed-phase LC have very strong elution strength in HILIC systems. Hence, the solvent of the first-dimension fraction is stronger than the second dimension mobile phase, either in HILIC-RP or in RP-HILIC 2D systems [38].

To solve the mobile phase compatibility issue in two-dimensional HPLC, it is necessary to investigate the effect of the sample volume and of the sample solvent on the separation under fast gradient conditions. Some time ago, Layne et al. [24] performed similar study on 2–5 cm long columns with gradient run times 4.5–7.5 min, which are however too long for a FIF or SIF second-dimension gradient operation. They observed impairing peak distortion when the concentration of acetonitrile as the sample solvent increased and suggested solving this problem by sample diluting with a weak solvent, adjusting gradient so that sample elutes at a longer elution time, or using a larger separation column. Unfortunately, neither of these remedies can be used in second-dimension fast gradient operation in on-line comprehensive LC × LC.

In this work, we studied the effects of the sample volume and of the concentration of aqueous acetonitrile as the sample solvent on separation under various fast second-dimension gradient conditions on a short (30 × 3 mm i.d.) column packed with fused-core porous shell Ascentis Express C18 particles (2.7 μm). We selected this type of column as it allows fast separation at a high flow rate and relatively moderate pressures (up to 400 bar), in contrast to fully porous columns enabling fast separations at very high pressures only. We compared the solvent effects on chromatographic behavior of benzene and homologous alkylbenzenes (C_1–C_5), to investigate the role of sample retention, which regularly increases with lipophilicity, i.e., with alkyl length in reversed-phase systems. This work was aimed to investigate the limits of sampling volume and solvent in the second dimension of comprehensive LC × LC, where relatively large effluent fractions in strong solvents may be transferred into the second dimension to provide fast separation and to avoid undersampling from the first dimension. Alkylbenzenes were selected as sample compounds with regularly increasing lipophilicity, which can be used to calibrate the retention scale in RP HPLC, and investigate the sample retention effects in combination with sample solvent and volume. On the other hand, the predicted retention volumes of alkylbenzenes can be used for the selection of the gradient range in second dimension. This approach can be applied to other compounds, which can be attributed certain equivalent to alkylbenzene polarity.

2. Theory

2.1. Retention times and bandwidths in gradient elution, gradient pre-elution and post-gradient elution

The retention in RP gradient elution can be predicted using the well-known linear solvent strength equation, if the instrumental dwell volume can be neglected and the isocratic retention can be described by simple equation:

$$\log k = a - m \cdot \varphi \quad (1)$$

where φ is the volume fraction of the organic solvent in aqueous–organic mobile phase. a is the (extrapolated) $\log k$ in pure water as the mobile phase, m is a measure of solvent strength of the organic solvent for a particular sample (change in $\log k$ per the change of organic solvent from 0 to 100%) [3,20–23,37].

Linear solvent strength gradients are applied most frequently to reversed-phase separations. Here, the volume fraction of the organic solvent in water, φ, increases in direct proportion to the time elapsed from the start of the gradient, t [20,21]:

$$\varphi = A + B.F_m.t \quad (2)$$

$B = (\varphi_f - A)/t_G$ is the gradient ramp (steepness), i.e., the change in the volume fraction of the organic solvent during the gradient run from the start, A, to the end, φ_f, of the gradient, which is often from 0 to 100% organic solvent with FIF gradients. t_G is gradient time, F_m is the flow rate of the mobile phase. Hence, the gradient concentration range can be optimized more efficiently with SIF or CS gradients.

For linear solvent strength gradients in reversed-phase systems described by Eq. (1), the elution times can be calculated using Eq. (3) [20–23]:

$$t_R F_m = \frac{t_G F_m}{m(\varphi_f - A)} \log\left[\frac{2.31m(\varphi_f - A)V_m 10^{(a-mA)}}{t_G F_m} + 1\right] + V_m \quad (3)$$

This equation describes adequately the gradient systems, where the sample migrates along the column only during the gradient run, i.e., the instrumental gradient dwell volume, V_D, can be either neglected, or just subtracted from the experimental elution volume. V_m is the column hold-up volume.

However, this is usually not the case with short columns and fast gradients, where isocratic gradient pre-elution may occur due to the inner volume of the high-pressure pump volume and connecting tubing to the sample injector, so-called "gradient dwell volume" (0.4–2 ml with common HPLC instruments). The dwell volume is filled with mobile phase at the start of the gradient and sample compounds may travel some distance along the column under isocratic conditions in the mobile phase originally contained in the instrumental dwell volume, until the gradient front reaches the actual analyte zone position in the column. In such a case, the contribution of the instrumental dwell volume to the elution time (volume) is important and some less retained sample compounds may even elute before the start of the gradient, in the gradient pre-elution step (1), especially with columns of a low inner volume. Even the elution times of analytes eluting in course of the gradient (2) or after the end of the gradient step (3) may be more or less affected by partial migration along the column before the gradient in the dwell-volume mobile phase [20,23,39]. According to the position of the sample zone in the column at the time it comes into contact with the front of the gradient, the remaining column volume available for the sample migration during the gradient is smaller than the total column volume. This situation should be respected in the calculation algorithm. As illustrated in Fig. 2, the retention can be described considering the three segments as 3 serially connected columns run under dwell-volume isocratic (1), gradient (2) and post-gradient isocratic (3) conditions. It should be noted that the relative contributions of the three steps to the retention may vary for individual analytes, depending on their retention on the column.

Some compounds may elute from the column before the gradient. The elution volumes, V_R, of compounds subject to pre-gradient elution within the dwell volume (possibly including an intentional initial isocratic hold-up step), $V_{init} = V_D + V_{hold}$ can be calculated as usual in isocratic elution, using the retention factor in the mobile phase contained in the dwell volume, k_{init}:

$$V_R = V_m(1 + k_{init}) \quad (4)$$

Other analytes move only along a part of the column during the pre-gradient step, corresponding to the proportional part, $V_{m,init}$, of the total column hold-up volume, V_m, but anyway this migration contributes to the total retention, as it diminishes the column hold-up volume available in the gradient step, $V_{m,g} = V_m - V_{m,init}$. The contribution of the gradient step to the retention, $t_{R,g}$, can be calculated from Eq. (3) using the diminished "gradient" hold-up volume, $V_{m,g}$, instead of V_m; however the dwell volume, V_D, should be included in calculations of the total gradient volume, V_R, affected by partial pre-gradient contribution. The solution yields Eq. (5) [3,20]:

$$V_R = \frac{1}{mB} \log\{2.31mB[V_m 10^{(a-mA)} - V_D] + 1\} + V_m + V_D \quad (5)$$

The contribution of the gradient step to the elution volume of a sample subject to post-gradient elution is equal to the total gradient volume, V_{post}, which adds to the contribution of the post-gradient isocratic elution, V_G, at the retention factor k_f in the volume fraction of the organic solvent at the end of the gradient, φ_f,

$$V_R = V_G + V_{post} = V_G + V_{m,post}(1 + k_f) \quad (6)$$

The proportional part of the column hold-up volume available for post-gradient elution can be determined after subtraction of the contribution of the gradient step and – if necessary – of the pre-gradient dwell step from the total column hold-up volume, V_m:

$$V_{m,post} = V_m - V_{m,g} - V_{m,init} \quad (7)$$

The contribution of the gradient step to the total column hold-up volume, $V_{m,g}$ can be calculated from Eq. (5) using the parameters of Eqs. (1) and (2), after setting $V_m = V_{m,g}$ and $V_R = V_G$ The post-gradient elution may often give rise to sample carry over in second-dimension gradients and should be therefore avoided. Eq. (6) can be used for this purpose, as it allows predicting post-gradient elution conditions.

Bandwidths in gradient elution, w_g, can be estimated as equal to isocratic bandwidths in the mobile phase at the elution time of peak maximum (at $\varphi = \varphi_e$), with instantaneous retention factor k_e, [3,20–23],

$$w_g = \frac{4 \cdot V_{m,g}(1 + k_e)}{\sqrt{N}} \quad (8)$$

considering:

$$k_e = 10^{(a - m \cdot \varphi_e)} \quad (9)$$

and:

$$\varphi_e = A + B \cdot (V_{R,g} - V_{m,g} - V_D) \quad (10)$$

For calculations of the gradient bandwidths, it is necessary to determine the column efficiency in terms of the number of theoretical plates, N. It should be stressed that the plate number cannot be calculated directly from the elution times and bandwidths measured in a gradient chromatogram. The height equivalent to theoretical plate (HETP) depends on the concentration of acetonitrile in the mobile phase, probably due to changing viscosity in two-component aqueous–organic mobile phases. This means that the column plate number and the HETP may change significantly during gradient elution. To account for changing column efficiency during a gradient run in calculations of w_g, either average plate number, or isocratic N in the mobile phase at the time of elution can be used in Eq. (8). In the present work we applied the second approach, which seems more appropriate, as the gradient sample zones are subject to compression during migration along the column at decreasing k and the actual bandwidth is largely controlled by the conditions at the time of elution. Exact calculations take into account corrections for additional gradient band compression due to the fact that the rear part of the sample zone migrates in stronger mobile phase, i.e. at slightly higher velocity, than the front part [21,22,40]. However, as the peaks are very narrow at fast gradient elution on a short efficient column, the additional band compression due to this effect should be very small, if any, and was neglected in this work.

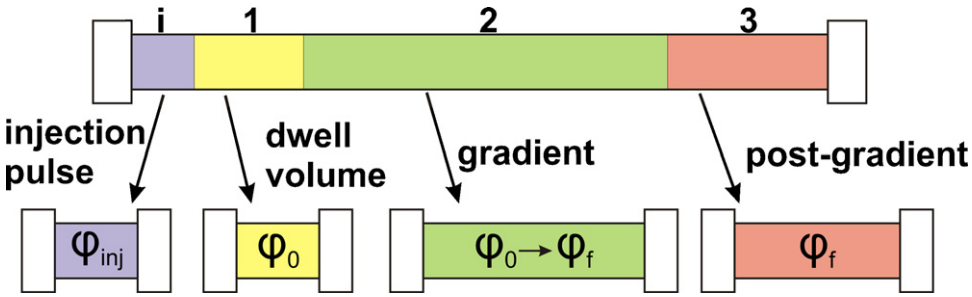

Fig. 2. Hypothetic scheme of pre-gradient dwell volume (1), gradient (2) and post-gradient (3) segments. Calculation of elution data as in serial (2) and isocratic (3) contributions to the total elution volume ($V_R = V_{R,init} + V_{R,G} + V_{R,post}$) and to the total column hold-up volume ($V_m = V_{m,init} + V_{m,G} + V_{m,post}$).

2.2. Effects of sample volume and solvent on the bandwidths and peak shape in gradient elution

When a large sample volume, V_{inj} (with respect to the column hold-up volume, V_m) is injected onto the column, the sample solvent acts as the mobile phase for some time, depending on the V_{inj} and on the sample retention factor in the solvent, k_{inj}. At the mass overload, strongly distorted (tailing) peaks may be observed due to non-linear isotherm distribution [41,42]. In the absence of column overload by the sample mass, the retention is controlled by linear isotherm and the minimum variance of a rectangular injection profile in isocratic elution, $\sigma^2_{inj} = V^2_{inj}/12$ [41]. In linear chromatography, the original sample volume may be either suppressed or enhanced, depending on the V_{inj} and k_{inj}.

If a large sample volume is injected in a weak eluting solvent, the sample molecules stay adsorbed on the top of the column in a narrow zone until they are taken over by the mobile phase with a high enough elution strength, so that the original width of the sample zone is suppressed and the injection volume has only minor effect on the retention times and bandwidths. This "sample focusing" effect is often used for improving the sensitivity by injecting large volumes of diluted samples (mainly in aqueous matrices).

However, after injection of a large volume of sample dissolved in a stronger eluent than the mobile phase, a part of the strong solvent may be adsorbed on the column, but a larger part of the solvent migrates along the column at the mobile phase velocity. This phenomenon affects the distribution of the sample molecules at different positions in the injected sample plug. The molecules at the rear edge of the injected pulse are immediately exposed to a weak mobile phase and move more slowly than the molecules inside the injected sample plug, which migrate along the column for a longer or a shorter time in the strong injection solvent zone at the velocity controlled by their retention factor in the sample solvent, k_{inj}, until they are taken over by the mobile phase. This effect is most apparent with sample molecules at the front edge of the injected pulse and may have significant impact on the width and shape of the sample bands at the time of elution.

The contribution of the volume of the injection pulse to the bandwidth at the time of elution, w_{pulse}, can be calculated as the difference between the migration times of the rear and the front parts of the injected sample plug at the time of elution [43]. The sample molecules at the front end of the sample plug migrate along the column in the mobile phase a shorter distance than the molecules at the rear end of the sample plug, because of their previous migration in the injection solvent. This means that the part of the column hold-up volume, $V_{m,mp}$, available for the migration of the sample molecules at the front end of the sample plug diminishes proportionally to the injected sample volume. This investigation was aimed to investigate the limits of sampling volume and solvent in the second dimension of comprehensive LC × LC, where relatively large effluent fractions in strong solvents may be transferred into the second dimension to provide fast separation and to avoid undersampling effects:

$$V_{m,mp} = V_m - V_{m,inj} = V_m - \frac{V_{inj}}{1 + k_{inj}} \tag{11}$$

If the sample is not retained at all in the sample solvent, $V_{m,inj} = V_{inj}$. For compounds eluting under isocratic conditions, such as in the dwell-volume step before the gradient, w_{pulse} can be calculated considering the differences between the distances migrated by the front and the rear sample plug in the injection solvent, k_{inj}, and in the mobile phase, k_i:

$$w_{pulse} = \frac{V_{inj}(1 + k_i)}{(1 + k_{inj})} \tag{12}$$

From Eq. (12) it follows that for a large k_{inj}, w_{pulse} can be neglected due to on-column "sample focusing". For samples injected in the mobile phase, $k_{inj} = k_i$ and the full injected pulse volume contributes to the bandwidth at the time of elution. On the other hand, for samples injected in strong solvents $k_{inj} < k_i$, which means that $V_{pulse} > V_{inj}$ and the bandwidth at the time of elution is subject to additional band broadening.

The sample volume and sample solvent effects in gradient elution are similar to isocratic elution, except for generally less broad peaks due to increasing elution strength during the gradient run (gradient band focusing), which affects the contribution of the injection pulse to the final bandwidth, w_{pulse}. Like in isocratic elution, the bandwidths of sample compounds injected in a large volume can be estimated as the difference between the retention of the rear end of the injection pulse, calculated from Eq. (5) and the retention of the plug front, calculated also from Eq. (5), but considering diminished part of the column hold-up volume available for gradient elution after the end of the sample migration in the injection solvent plug, $V_{m,G}$, that should be used instead of V_m:

$$V_{m,G} = V_m - V_{m,inj} \tag{13}$$

This approach yields Eq. (14) for the sample plug contribution to the gradient bandwidth:

$$w_{pulse} = \frac{1}{mB} \log \frac{2.31mB[V_m 10^{(a-mA)} - V_D] + 1}{2.31mB\left[\left(V_m - \frac{V_{inj}}{1+k_{inj}}\right) \cdot 10^{(a-mA)} - V_D\right] + 1} + \frac{V_{inj}}{1 + k_{inj}} \tag{14}$$

Like in isocratic LC, the contribution of the injected pulse, V_{inj}, can be neglected at large sample k_{inj} and sample focusing is observed. Band suppression (gradient focusing) due to increasing elution strength during the gradient run acts against the opposite band broadening effect of the sample plug volume and Eq. (14) can be used to estimate the result of the two effects on the eventual gradient bandwidths. Unfortunately, gradient focusing cannot compensate band

broadening due to large sample volumes injected in strong eluting solvent, in which k_{inj} is very low (such as in 100% acetonitrile).

The total sample bandwidth in gradient elution of large sample volumes can be roughly estimated as the sum of the contributions of the sample plug contribution calculated from Eq. (14) and of the regular 4σ band broadening at the injection of a narrow sample pulse (e.g., 1 μL), w_g, calculated from Eq. (8):

$$w_{est} = w_g + w_{pulse} \quad (15)$$

It should be noted that Eq. (15) is not theoretically rigorous and may be used to estimate the effect of the injected sample volume on the band broadening, but it does not provide any information on the actual band shape, which may be distorted or split due to changing conditions during the sample plug migration along the column.

When large sample volumes are injected, w_{pulse} may become larger than the column hold-up volume for some sample compounds, which may not be retained at all and migrate along the whole column length in a strong solvent zone, until they appear in the effluent at the breakthrough volume of the solvent, close to the column hold-up time. This effect causes significant band distortion and splitting and should be avoided, as it may destroy the separation.

3. Experimental

3.1. Materials and reagents

The Ascentis Express C18 column, 2.7 μm fused core particles, 0.5 μm porous-shell outer layer, 30 × 3.0 mm i.d., was obtained from Supelco (Bellafonte, PA, USA). Acetonitrile, LiChrosolv grade, was purchased from Merck (Darmstadt, Germany). Water was purified using a SG Ultra Clear UV water purification system (SG, Hamburg, Germany). The mobile phases were filtered using a Millipore (Bedford, MA, USA) 0.45-μm filter and degassed by ultrasonication before use.

n-Alkylbenzene standards (from benzene to n-pentylbenzene) were obtained from Sigma–Aldrich (St. Louis, MI, USA). The stock solutions of standards (20 g/L) were prepared in acetonitrile. The working standard solutions were obtained by dilution with the mobile phase or other injection solvents as appropriate. The concentrations of the samples injected into the liquid chromatograph were 0.16 g/L.

3.2. Equipment

A 1100 Liquid Chromatograph (Agilent, Palo Alto, CA, USA) equipped with a micro-flow binary pump, a degasser, an auto-sampler, a diode-array UV detector set to 254 nm and a thermostatted column compartment was used in the experiments.

3.3. Methods

The isocratic retention data used for the determination of the parameters a, m of Eq. (1) listed in Table 1 were measured under isocratic conditions in pre-mixed mobile phases at different concentrations of acetonitrile in aqueous–organic mobile phases at the flow-rate of 0.5 mL/min. All gradient experiments were performed at 4.5 mL/min. The temperature was set to 40 °C in all isocratic and gradient experiments. The column hold-up volume (V_m = 0.16 mL) was measured as the elution volume of uracil as non-retained marker. The gradient delay volume (V_D = 1.15 mL) was measured by running a linear gradient of 0.1% acetone in acetonitrile in pure acetonitrile [21].

Table 1
Parameters a, m of Eq. (1) determined as the best fit parameters of experimental $\log k - \varphi$ plots of alkylbenzene; column: Ascentis Express C18, 30 × 3.0 mm, 2.7 μm (V_m = 0.16 mL, ε_T = 0.74). SD, standard deviation; R^2, correlation coefficients.

No.	Compound	m	SD	a	SD	R^2
1	Benzene	2.64	0.06	1.62	0.03	0.999
2	Methylbenzene	3.05	0.09	2.05	0.04	0.999
3	Ethylbenzene	3.45	0.13	2.47	0.06	0.999
4	Propylbenzene	3.90	0.15	2.93	0.08	0.998
5	Butylbenzene	4.36	0.19	3.40	0.10	0.998
6	Pentylbenzene	4.79	0.22	3.85	0.11	0.998

4. Results and discussion

4.1. Calculations of the retention data in fast gradient elution

To test the validity of the theory developed with conventional gradients for the retention behavior with steep gradients run in 1 min, we measured chromatograms of benzene and alkylbenzenes on a short (3 cm) the porous-shell Ascentis Express C18 column with various fast (1 min) gradients of acetonitrile in water at a high flow-rate of the mobile phase (4.5 mL/min) at 40 °C. To avoid the effect of the injection volume on the results, we injected 1 μL samples in this series of experiments. The gradient range was selected to represent the full concentration change from 0 to 100% acetonitrile, usual in FIF second-dimension gradients and narrower concentration ranges (20–100% acetonitrile, 50–100% acetonitrile, 2–50% acetonitrile and 15–50% acetonitrile), representing high and low mobile phase elution strength segments of SIF second dimension gradients. The experimental elution times and bandwidths are compared with the data predicted by calculation in Table 2. The calculations were based on the parameters a, m of Eq. (1) determined in isocratic experiments (Table 1).

The elution volumes were calculated using Eq. (5), taking into account possible partial contribution of sample migration along the column in the dwell-volume pre-gradient isocratic step 1, except for benzene, methylbenzene and ethylbenzene in the high concentration range gradient from 50 to 100% acetonitrile, which elute during the dwell-volume isocratic step 1(a). Their elution data were calculated as usual in isocratic elution, using Eq. (4). In 1-min gradients from 0 to 100% acetonitrile and from 20 to 100% acetonitrile, all peaks elute in the gradient range (step 2 in Fig. 2). On the other hand, in low-concentration range gradients, propylbenzene, butylbenzene and pentylbenzene elute after the end of the gradient step with elution times higher than 1.29 min, corresponding to the sum of the gradient time, column hold-up time and dwell-volume time. Their elution times were calculated using Eq. (6). The calculated elution times were 0.01–0.06 min higher than the experimental values, except for the compounds eluted after the end of gradient. These minor systematic differences, in addition to common experimental errors, could be possibly attributed to that the parameters a, m, of Eq. (1), used in calculations of the gradient retention data from Eq. (5), were measured under isocratic conditions in premixed two-component mobile phases, whereas during the gradient elution acetonitrile is mixed with water directly in the instrument. Anyway, the results suggest suitability of the calculation approach for prediction of retention in fast gradients. This approach should be particularly useful in optimization of second-dimension LC × LC gradients, as it enables determination of the useful gradient concentration range for separation of samples within specified retention range, controlled by sample lipophilicity [18].

A constant flow rate of 2.5 ml/min was used in all experiments, far above the minimum of the Van Deemter curve, because fast separation was required. The volume fraction of acetonitrile in the mobile phase, φ, affects the diffusion coefficients and consequently the column efficiency. Hence, we investigated the effect of

Table 2
Experimental (exp) and calculated (calc) retention data of alkylbenzenes; column: Ascentis Express C18 30 × 3 mm, 2.7 μm; flow rate, 4.5 mL/min; temperature, 45 °C; B, benzene; MB, methylbenzene; EB, ethylbenzene; PrB, propylbenzene; BB, butylbenzene; PnB, pentylbenzene; V_R, elution volume; k_e, retention factor at the time of elution of peak maximum; φ_e, concentration of acetonitrile at the time of elution of peak maximum; w_t, peak width. Injection: 1 μl sample dissolved in the mobile phase used at the start of the gradient.

Gradient	Comp.	$t_{R(exp)}$ (min)	$t_{R(calc)}$ (min) (Eq. (5))	$k_{0(calc)}$ (Eq. (1))	$k_{e(calc)}$ (Eq. (9))	φ_e (%.10^{-2}) (Eq. (10))	$w_{t(exp)}$ (min)	$w_{t(calc)}$ (min) (Eq. (8))
0–100% ACN in 1 min	B	0.61	0.64	41.9	5.03	0.28	0.010	0.014
	MB	0.71	0.76	112	4.22	0.42	0.010	0.011
	EB	0.78	0.84	293	3.66	0.52	0.010	0.010
	PrB	0.86	0.91	850	3.22	0.60	0.012	0.009
	BB	0.92	0.96	2509	2.87	0.66	0.012	0.008
	PnB	0.98	1.01	7074	2.61	0.71	0.012	0.008
20–100% ACN in 1 min	B	0.39	0.42	12.4	6.38	0.28	0.014	0.017
	MB	0.53	0.58	27.6	5.52	0.39	0.013	0.014
	EB	0.63	0.69	59.7	4.74	0.47	0.012	0.012
	PrB	0.72	0.78	141	4.10	0.54	0.014	0.011
	BB	0.80	0.86	336	3.62	0.61	0.013	0.010
	PnB	0.87	0.91	780	3.28	0.67	0.013	0.009
50–100% ACN in 1 min	B[a]	0.09	0.10	2.01	2.01	0.50	0.010	0.009
	MB[a]	0.13	0.15	3.36	3.36	0.50	0.011	0.012
	EB[a]	0.20	0.22	5.49	5.49	0.50	0.014	0.015
	PrB	0.31	0.36	9.56	6.59	0.51	0.018	0.017
	BB	0.43	0.48	16.6	6.19	0.57	0.018	0.016
	PnB	0.54	0.58	28.6	5.59	0.63	0.019	0.014
2–50% ACN in 1 min	B	0.75	0.77	37.1	9.20	0.24	0.022	0.023
	MB	0.99	1.02	97.5	8.44	0.36	0.020	0.020
	EB	1.16	1.21	250	7.53	0.44	0.020	0.017
	PrB[b]	1.33	1.28	710	9.56	0.50	0.025	0.022
	BB[b]	1.58	1.55	2053	16.58	0.50	0.040	0.037
	PnB[b]	1.99	1.98	5674	28.59	0.50	0.067	0.065
15–50% ACN in 1 min	B	0.52	0.54	16.9	9.73	0.20	0.024	0.024
	MB	0.80	0.82	39.2	10.50	0.29	0.026	0.025
	EB	1.03	1.08	88.9	9.99	0.38	0.024	0.022
	PrB[b]	1.24	1.22	221	9.56	0.50	0.025	0.021
	BB[b]	1.50	1.49	556	16.58	0.50	0.039	0.036
	PnB[b]	1.92	1.93	1354	28.59	0.50	0.061	0.064

[a] . . .gradient pre-elution in the isocratic dwell-volume step.
[b] . . .elution after gradient, t_R calculated using Eq. (6).

the concentration of ACN in the mobile phase on band broadening of alkylbenzenes on the porous-shell Ascentis Express C18 column under isocratic conditions, to justify the selection of appropriate column efficiency for calculation of gradient bandwidths. Fig. 3(A) shows that the assumption of a constant HETP generally adopted for calculations of gradient bandwidths is not very realistic with fast gradients. We used the plate number, N, in the mobile phase at the time of elution of peak maxima ($\varphi = \varphi_e$), determined from the plots in Fig. 3(B), and corresponding values of k_e for calculations of the bandwidths in gradient elution from Eq. (8), Using this approach, the predicted peak widths were in agreement with the experiment, with differences of 0.004 min or less (Table 2). The exact calculations of bandwidths should allow more realistic estimate of second-dimension gradient peak capacity.

4.2. Effects of the injection volume and sample solvent on the chromatographic behavior

The main objective of the present work was to investigate the effects of two crucial factors of sample transfer in comprehensive 2D LC × LC on possible band broadening, namely the volume of sample fractions and of the sample solvent, i.e., the mobile phase used in the first dimension. As the separation in the second dimension should be fast and efficient, we employed a short fused-core porous

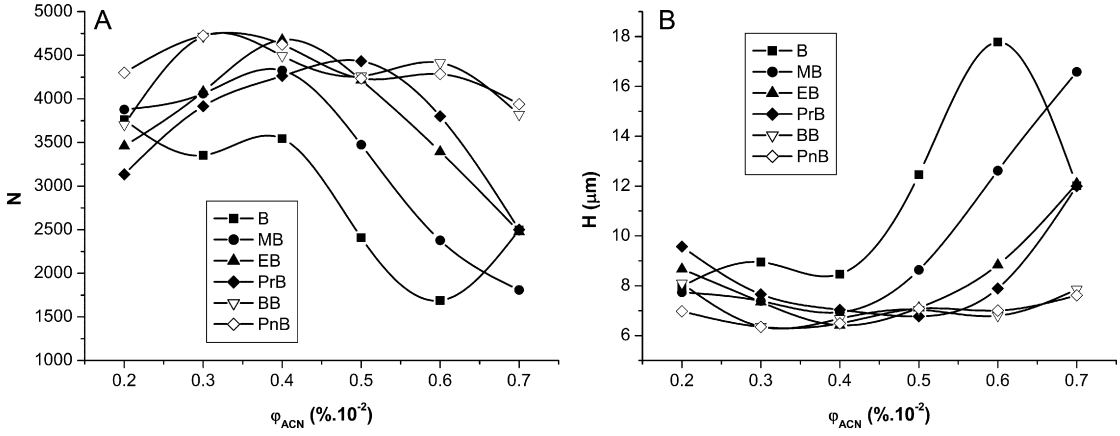

Fig. 3. Effects of the concentration of acetonitrile in the mobile phase (isocratic) on the height equivalent to a theoretical plate (HETP) and on the plate number, N, for an Ascentis Express C18 30 × 3.0 mm 2.7 μm column. T = 40 °C; F_m = 4.5 mL/min.

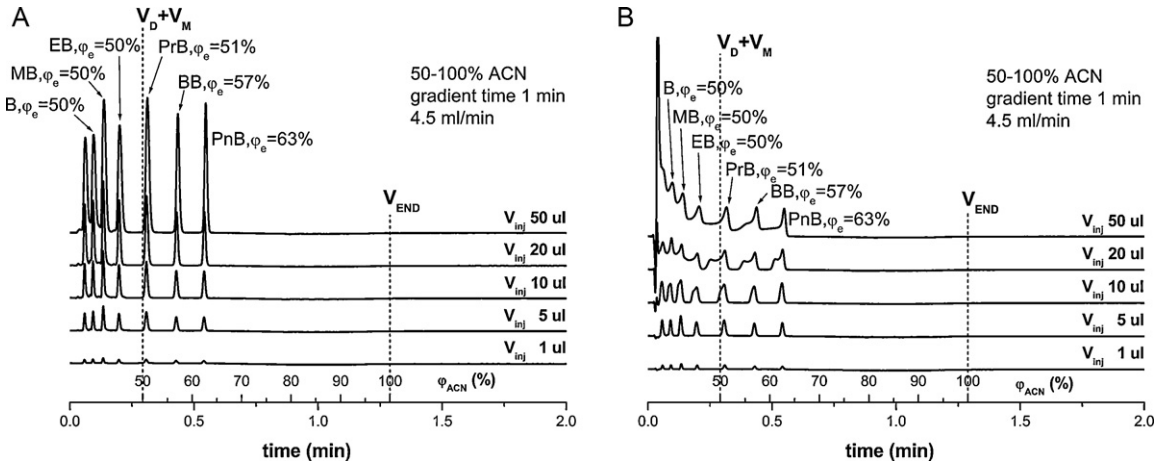

Fig. 4. Effects of the injection volumes (1–50 μL) and of the sample solvent on the separation of benzene and alkylbenzenes in a simulated SIF gradient (50–100% ACN in 1 min). (A) Sample in 50% acetonitrile; B, sample in 100% acetonitrile. Column Ascentis Express C18 30 × 3.0 mm 2.7 μm, 40 °C, 4.5 mL/min. Dashed lines separate pre-gradient, in-gradient and post-gradient elution segments. Concentrations of acetonitrile at the time of elution are given at the peaks of benzene (B), methylbenzene (MB), ethylbenzene (EB), propylbenzene (PrB), butylbenzene (BB) and pentylbenzene (PnB).

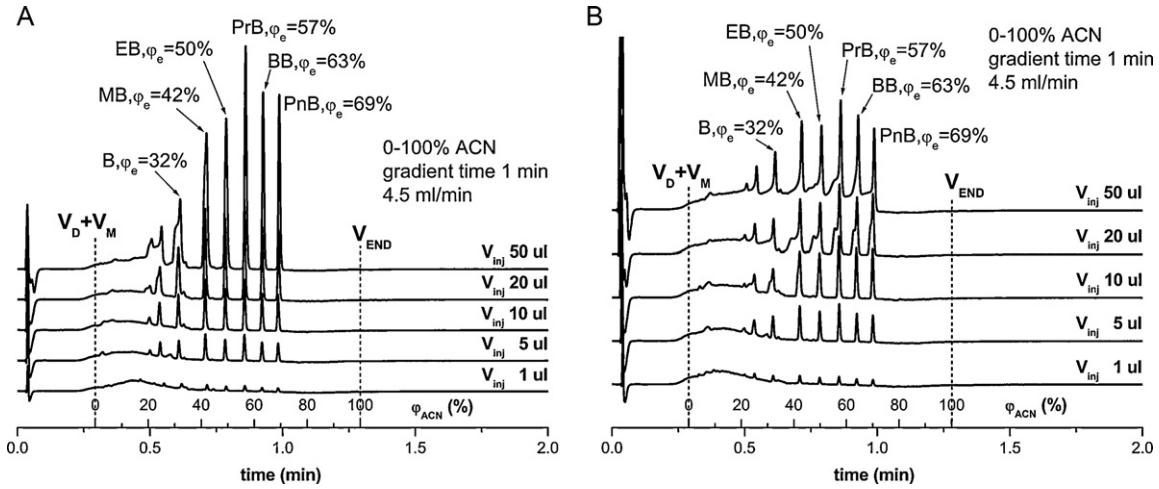

Fig. 5. Effects of the injection volumes (1–50 μL) and of the sample solvent on the separation of benzene and alkylbenzenes in a simulated FIF gradient (0–100% ACN in 1 min). (A) Sample in 50% acetonitrile; (B) sample in 100% acetonitrile. Column: Ascentis Express C18 30 × 3.0 mm 2.7 μm, 40 °C, 4.5 mL/min. Dashed lines separate pre-gradient, in-gradient and post-gradient elution segments. Concentrations of acetonitrile at the time of elution are given at the peaks of benzene (B), methylbenzene (MB), ethylbenzene (EB), propylbenzene (PrB), butylbenzene (BB) and pentylbenzene (PnB).

shell column, fast 1 min gradients at a high flow rate (4.5 ml/min), These conditions are much less favorable to accommodate relatively large samples dissolved in strong eluting solvent than less steep gradients run at lower flow-rates in conventional gradient LC, but correspond to the practice of second-dimension reversed-phase systems, providing good performance in 2D LC × LC [18]. It can be assumed that the sample volume and sample solvent effects in one-dimensional LC will affect the separation less seriously. The selection of homologous alkylbenzenes as samples allows investigate the solvent effects with samples of different retention, which regularly increases with increasing lipophilicity at longer alkyl lengths.

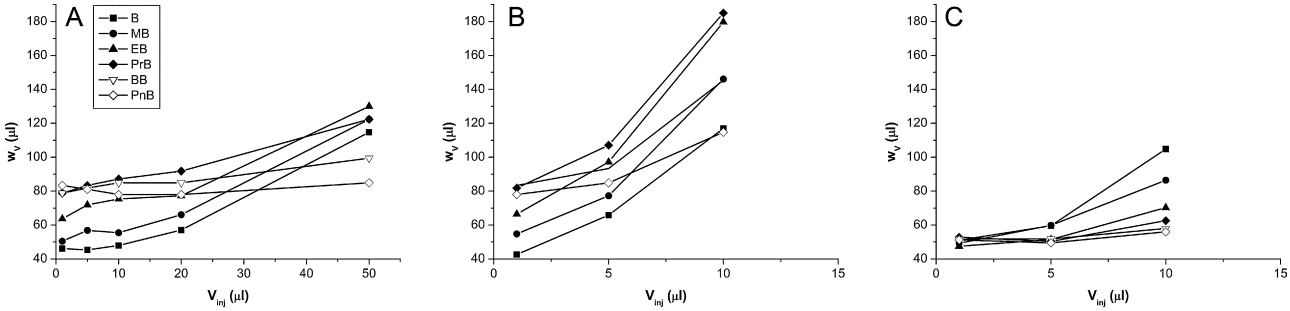

Fig. 6. Effects of the sample volume, V_{inj}, and sample solvent on the bandwidths, w, of alkylbenzenes, (A) sample in 50% acetonitrile, gradient 50–100% acetonitrile in 1 min; (B) sample in 100% acetonitrile, gradient 50–100% acetonitrile in 1 min; (C) sample in 100% acetonitrile, gradient 0–100% acetonitrile in 1 min. Column Ascentis Express C18 30 × 3.0 mm 2.7 μm, 40 °C, 4.5 mL/min.

Table 3
Experimental peak widths, $w_{t(exp)}$, and peak width calculated from the difference between the elution times of the start and end of the injection pulse, $w_{t(pulse)}$ from Eq. (14), estimated total bandwidths, $w_{t(est)}$, calculated from Eq. (15). V_{inj}, volume of injected sample; sample injected in 50% ACN. Column: Ascentis Express C18, 30 × 3.0 mm 2.7 μm, flow rate 4.5 mL/min, temperature 45 °C; B, benzene; MB, methylbenzene; EB, ethylbenzene; PrB, propylbenzene; BB, butylbenzene; PnB, pentylbenzene.

Gradient	Comp.	V_{inj} (μL)					
		20			50		
		$w_{t(pulse)}$ (min)	$w_{t(est)}$ (min)	$w_{t(exp)}$ (min)	$w_{t(pulse)}$ (min)	$w_{t(est)}$ (min)	$w_{t(exp)}$ (min)
0–100% ACN in 1 min	B	0.009	0.023	0.016	0.024	0.038	0.033
	MB	0.005	0.016	0.014	0.014	0.025	0.025
	EB	0.003	0.013	0.013	0.008	0.018	0.018
	PrB	0.002	0.011	0.012	0.005	0.014	0.013
	BB	0.001	0.009	0.012	0.002	0.010	0.012
	PnB	0.001	0.009	0.012	0.001	0.009	0.013
20–100% ACN in 1 min	B	0.012	0.029	0.030	0.030	0.047	0.056
	MB	0.007	0.021	0.016	0.017	0.031	0.034
	EB	0.004	0.016	0.014	0.010	0.022	0.021
	PrB	0.002	0.013	0.013	0.005	0.016	0.016
	BB	0.001	0.011	0.013	0.003	0.013	0.014
	PnB	0.001	0.010	0.013	0.002	0.011	0.014
50–100% ACN in 1 min	B[a]	0.004	0.013	0.013	0.011	0.020	0.025
	MB[a]	0.004	0.016	0.015	0.011	0.023	0.027
	EB[a]	0.004	0.019	0.017	0.011	0.026	0.029
	PrB	0.003	0.020	0.020	0.009	0.026	0.027
	BB	0.002	0.018	0.019	0.005	0.021	0.022
	PnB	0.001	0.015	0.017	0.003	0.017	0.019

[a] Gradient pre-elution in the isocratic dwell-volume step.

We investigated the effect of the volume of samples containing benzene and methylbenzene to pentylbenzene dissolved in 50% and in 100% acetonitrile on the band broadening and peak splitting on a porous-shell Ascentis Express C18 column, 30 × 3 mm, in fast 1 min gradients (4.5 ml/min). 50% acetonitrile represents the sample solvent in the fractions from a reversed-phase first-dimension system, whereas 100% acetonitrile is close to the sample solvent in the fractions transferred from a HILIC first-dimension solvent. We did not observe any apparent effect of the sample concentration on bandwidths when injecting 1 μL samples containing 0.16–20 g/L of each benzene and C_1–C_5 alkylbenzenes, which rules out mass overload effects on the retention when changing the volumes of samples containing 0.16 g/L of sample compounds from 1 to 50 μL. Chromatograms obtained with various injected sample volumes are shown in Fig. 4 for gradients 50–100% acetonitrile, characteristic for second-dimension SIF gradients, and in Fig. 5 for gradients 0–100% acetonitrile, typical for second-dimension FIF gradients in coupled two-dimensional LC × LC systems. The broken vertical lines separate the pre-gradient, the gradient and the post-gradient elution range. The chromatograms show that the elution times and the acetonitrile concentrations at the elution of peak maxima, φ_e, – Eq. (10) – are practically independent of the injected sample volume and solvent. 1-μL volumes of samples dissolved in 100% acetonitrile show very similar bandwidths as the same sample volumes in 50% acetonitrile. However, the bandwidths increase with increasing sample volume, depending on the retention times of analytes controlled by their alkyl lengths and gradient conditions (Fig. 6).

In 50–100% acetonitrile gradient, the bandwidths of sample compounds dissolved in 50% acetonitrile (the mobile phase at the start of the gradient) increase with increasing sample retention, i.e.,

Table 4
Experimental peak widths, $w_{t(exp)}$, and peak width calculated from the difference between the elution times of the start and end of the injection pulse, $w_{t(pulse)}$ from Eq. (14), estimated total bandwidths, $w_{t(est)}$, calculated from Eq. (15). V_{inj}, volume of injected sample; sample dissolved in 100% ACN. Column Ascentis Express C18, 30 × 3.0 mm 2.7 μm, flow rate, 4.5 mL/min; temperature, 40 °C; B, benzene; MB, methylbenzene; EB, ethylbenzene; PrB, propylbenzene; BB, butylbenzene; PnB, pentylbenzene.

Gradient	Comp.	V_{inj} μL)					
		20			50		
		$w_{t(est)}$ (min)	$w_{t(pulse)}$ (min)	$w_{t(exp)}$ (min)	$w_{t(est)}$ (min)	$w_{t(pulse)}$ (min)	$w_{t(exp)}$ (min)
0–100% ACN in 1 min	B	0.029	0.015	[b]	0.080	0.066	[b]
	MB	0.025	0.014	0.030	0.068	0.057	[b]
	EB	0.022	0.012	0.024	0.060	0.050	0.059
	PrB	0.020	0.011	0.018	0.054	0.045	0.057
	BB	0.018	0.010	0.021	0.050	0.042	0.056
	PnB	0.017	0.009	0.019	0.046	0.038	0.054
20–100% ACN in 1 min	B	0.035	0.018	[b]	0.098	0.081	[b]
	MB	0.031	0.017	[b]	0.087	0.073	[b]
	EB	0.027	0.015	0.039	0.075	0.063	0.077
	PrB	0.024	0.013	0.030	0.067	0.056	0.067
	BB	0.022	0.012	0.022	0.060	0.050	0.062
	PnB	0.020	0.011	0.020	0.055	0.046	0.060
50–100% ACN in 1 min	B[a]	0.013[a,b]	0.004	[b]	0.033	0.024	[b]
	MB[a]	0.019[a,b]	0.007	[b]	0.048	0.036	[b]
	EB[a]	0.029[a,b]	0.014	[b]	0.072	0.057	[b]
	PrB	0.036	0.019	0.055	0.100	0.083	[b]
	BB	0.034	0.018	0.041	0.096	0.080	[b]
	PnB	0.031	0.017	0.028	0.087	0.073	[b]

[a] Gradient pre-elution in the isocratic dwell-volume step.
[b] Distorted peaks.

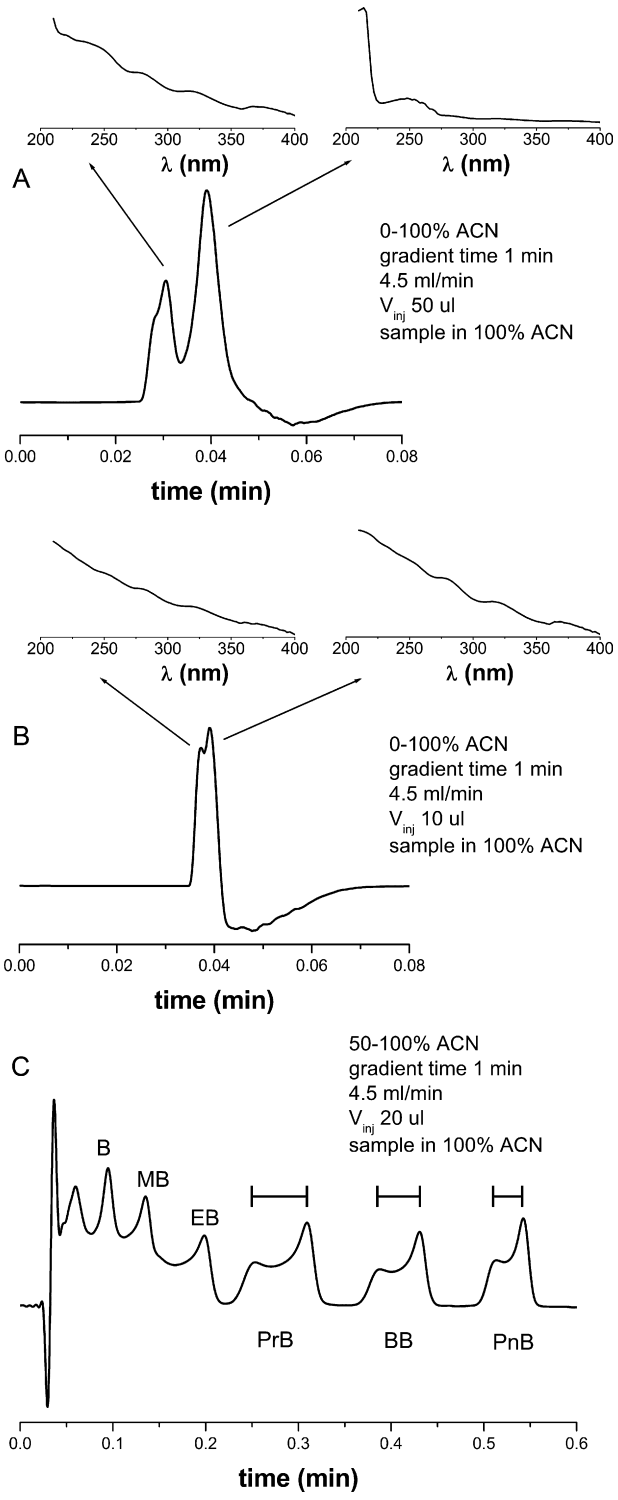

Fig. 7. Band distortion and splitting of sample injected in solvent with incompatible elution strength (100% ACN). Gradient 0–100% acetonitrile in 1 min. (A) breakthrough peak of acetonitrile and of benzene (alkylbenzenes), V_i = 50 μL; (B) breakthrough of acetonitrile only, V_i = 10 μL; (C) distorted peaks of propyl-, butyl- and pentylbenzene at the injection of 20 μL samples dissolved in 100% acetonitrile. Column Ascentis Express C18 30 × 3.0 mm 2.7 μm, T = 40 °C, 4.5 mL/min.

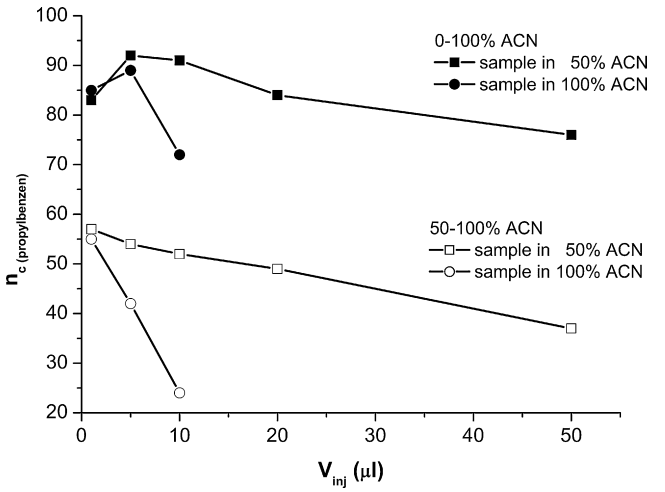

Fig. 8. Sample volume and solvent effect on gradient peak capacity, n_c, calculated as the gradient time, 1 min, divided by average bandwidth of propylbenzene (top) and gradient peak capacity related to the maximum peak capacity for V_{inj} = 1 μL (bottom). Distorted peaks are not considered.

for higher alkylbenzenes in low-volume samples (1–10 μL). Further increase in the bandwidths with increasing injected sample volume from 10 to 50 μL is much less significant for more retained butylbenzene and pentylbenzene, eluting during the gradient, than for weakly retained benzene and lower alkylbenzenes, which elute before the gradient in the isocratic dwell volume step at $V_R < V_D + V_m$ (Figs. 4(A) and 6(A)). Increasing the injection volumes of samples dissolved in 100% acetonitrile from 1 μL to 5 and 10 μL causes significant broadening of the bandwidths of all sample compounds in gradients from 50% to 100% acetonitrile (Figs. 4(B) and 6(B)); further increase in the injection volume to 20 and 50 μL causes band distortion and splitting (Fig. 7). Injection of sample volumes, larger than 10 μL dissolved in 100% acetonitrile, results in distorted elution profiles of all alkylbenzenes, strongly fronting and relatively sharp rear ends at the same elution times as 1 μL samples (Fig. 7(C)). The peaks of later eluting alkylbenzenes are split and the peaks of benzene to ethylbenzene co-elute (Fig. 4(B)).

In full-range (0–100% acetonitrile) gradients, all sample compounds elute during the gradient step (Fig. 5). These gradients show lower contributions of the injected volume to the bandwidths of alkylbenzenes than the gradients starting at higher acetonitrile concentrations (Fig. 6(C)), obviously due to more significant gradient band suppression effects over broad mobile phase composition range. Peak distortion and splitting were observed only for benzene and methylbenzene in samples dissolved in 50% acetonitrile at the injection volumes larger than 10 μL (Fig. 5(A)). 10 μL samples of earlier eluting analytes (benzene to propylbenzene) dissolved in 100% acetonitrile eluted as slightly fronting peaks, but more or less significant peak splitting was observed for all analytes injected in 20 μL and 50 μL samples (Fig. 5(B)), however the peak distortion and splitting were less strong than with the gradients starting at 50% acetonitrile (Fig. 4(B)).

Tables 3 and 4 show the experimental gradient bandwidths, $w_{t,exp}$, the predicted contributions of the injection volume to the bandwidths, $w_{t,pulse}$ (calculated from Eq. (14) for compounds eluting in the gradient step and from Eq. (12) for the compounds eluting before the gradient, in the isocratic dwell-volume step) and the estimated final bandwidths, $w_{t,est}$ (calculated as the sum of the band dispersion and the sample volume contribution, Eq. (15)) for various gradients and sample volumes. The band broadening increases with gradients starting at higher concentrations of acetonitrile. Taking into account simplifications adopted in the calculation approach, the estimated bandwidths are in relatively good agreement with the experimental bandwidths, $w_{t(exp)}$, especially for higher alkylbenzenes eluted in the gradient step. The data illustrate decreasing contributions of the injection pulse to the final bandwidths of higher alkylbenzenes injected both in 50% acetonitrile (Table 3) and in 100% acetonitrile (Table 4) in all gra-

dients tested. The maximum contributions of the sample volume injected in 50% acetonitrile to the bandwidths of butylbenzene and pentylbenzene eluting in the gradient step are equal to the injection pulse time, $w_{t,pulse} = t_i$ (0.004 min for V_i = 20 μL and 0.011 min for V_i = 50 μL). These contributions are larger for less retained benzene, methylbenzene and ethylbenzene, eluting before the gradient under isocratic dwell-volume conditions – Table 3.

The estimated final bandwidths for benzene injected in 50 μL 50% acetonitrile in gradients starting at 0% or 20% acetonitrile exceed the column hold-up time (0.035 min, corresponding to the column hold-up volume, V_m = 160 μL) – Table 3. At these conditions, the sample breakthrough occurs at the hold-up volume, which causes band splitting of the benzene peak (Figs. 5(A) and 7(C).

This effect, $w_{t(pulse)} > 0.035$ min, is predicted for all compounds dissolved in 100% acetonitrile and injected in 50 μL samples eluted in the gradient step at all gradient conditions studied (Table 4). These sample compounds pass through the column in the acetonitrile zone without retention and appear close to the column hold-up time, as show the typical aromatic absorption bands with maxima at 254 nm in the UV spectra of non-retained second peak (Fig. 7(A)). At lower sample volumes, the aromatic band was not observed in the breakthrough peak, which can be attributed to acetonitrile only (Fig. 7(B)), like the first peak in Fig. 7(A). (The UV absorption regularly decreasing with increasing wavelength can be probably attributed to the "viscous fingering" effect, causing imperfect mixing of the zones of acetonitrile and of more water-rich mobile phases at the early stage of the gradient elution, resulting in dispersion or refraction of the UV radiation in the detection cell, explaining thus the appearance of the first "hold volume peak").

The hold-up volume breakthrough was observed only for benzene in 50 μL samples dissolved in 50% acetonitrile, in gradients starting at 0% and 20% acetonitrile, but for all analytes dissolved in 100% acetonitrile, injected in 50 μL volumes at all gradient conditions; in gradients from 50 to 100% acetonitrile, the hold-up volume breakthrough occurs for propylbenzene and butylbenzene at 20 μL or larger injected sample volumes (Fig. 7(C)).

Large sample volume injected in strong eluent may significantly decrease the gradient peak capacity, n_c, with strong impact on the number of peaks actually resolved in the second dimension of 2D LC × LC systems showing poor mobile phase compatibility. The reason is that large sample volumes fill larger proportion of the column volume (and column length), so that lower plate number is available for separation, causing larger band dispersion and broader peaks. Fig. 8 illustrates the sample volume effect on the peak capacity of samples dissolved in 50% and in 100% acetonitrile in gradients starting in pure water and at 50% acetonitrile calculated as the number of peaks of propylbenzene (for the simplicity sake) that can fill the 1 min gradient elution space when stacked side-by-side (Fig. 8(top)) and as the percentual decrease in the maximum peak capacity (at 1 μL injection, Fig. 8(bottom)). The time necessary for column re-equilibration is not considered. It is clear that increasing sample volume and increasing concentration of acetonitrile in the sample solvent strongly decrease the gradient peak capacity, even when sample are not strongly distorted or split (such samples are not included in the plots in Fig. 8).

5. Conclusions

1. Conventional theory of gradient elution enables predictive calculations of elution times and bandwidths in fast gradients necessary for second-dimension operation of comprehensive LC × LC. The calculations are possible for compounds eluted in the gradient step, before the gradient at isocratic conditions in the dwell-volume mobile phase and after the end of the gradient. Calibration of the retention scale with homologous alkylbenzene series with gradually increasing lipophilicity enables selecting the upper limit of the concentration of organic solvent for second-dimension gradients, to suit the sample polarity range and to avoid pre-gradient and post-gradient elution, which could decrease the resolution, impair the regularity of the coverage of the retention plain or even cause undesired sample cross-over (warp-around) with second-dimension gradients in 2D LC × LC.
2. Short fused-core porous shell columns provide high flow-rate such as 4.5 mL/min at relatively moderate pressures up to 400 bar, within the limits of conventional HPLC instrumentation and therefore can be recommended for fast gradient second-dimension operation in very short separation times at high flow rates, rather than fully porous columns, which would allow fast separations only at very high pressures.
3. The limits of sampling volume and fraction solvent in the second dimension of comprehensive LC × LC were studied in detail, as relatively large effluent fractions in strong solvents are often transferred into the second dimension to provide fast separation and to avoid undersampling effects. Calculations of the elution times of the front-end and of the rear end of the injected sample plugs allow estimating the effects of the sample volume on the gradient bandwidths, even when using different sample solvents than the mobile phase at the start of the gradient. Generally, a weaker sample solvent tends to suppress sample bandwidths due to the on-column sample focusing effect, but using a stronger elution mobile phase in the first dimension than in the second one unfortunately cannot be avoided in some cases, such as when coupling orthogonal NP × RP or HILIC × RP 2D systems, but even in some combined RP × RP systems with different elution strengths of the mobile phases. The mismatch in the mobile phase strengths may cause incompatibility of the first-dimension and second-dimension separation conditions, as the first-dimension mobile phase is used as the fraction solvent to transfer the effluent fractions into the second dimension and may cause band broadening and even distortion or splitting.
4. The band broadening and the band splitting effects strongly decrease the column peak capacity and impair with increasing sample volume and increasing differences in the elution strength of the sample solvent and the mobile phase at the start of the gradient. With reversed-phase fast gradients, the sample volume effects are more critical for more polar (less retained) analytes than for the more retained ones. Even though the simplified calculation approach cannot predict the exact band shapes under the mobile phase mismatch conditions, it at least allows estimating and avoiding conditions at which sample compounds of various polarities may penetrate from the column in the breakthrough volume close to the column hold-up time.
5. To avoid detrimental band broadening and band distortion effects, as small as possible sample volumes should be injected, which means that small-volume fractions should be transferred from the first to the second dimension. With the shell-pore short 3 cm second-dimension column used in the present work, injection of sample volumes up to 5 μL, representing approximately 3% of the column void (hold-up) volume did not impair significantly the band broadening in fast 1 min gradients, but with more polar compounds, probably even lower fraction volumes should be used, especially in direct on-line coupling of HILIC and RP systems.

Acknowledgments

This work was supported by the Grant Agency of the Czech Republic, project 203/07/0641 and by the Ministry of Education, Youth and Sports of the Czech Republic, research project MSM 0021627502.

References

[1] Cs. Horváth, S.R. Lipsky, Anal. Chem. 39 (1967) 1993.
[2] U.D. Neue, J.L. Carmody, Y.-F. Cheng, Z. Lu, C.H. Phoebe, T.E. Wheat, Adv. Chromatogr. 41 (2001) 93.
[3] P. Jandera, Adv. Chromatogr. 43 (2005) 1.
[4] U.D. Neue, J. Chromatogr. A 1079 (2005) 153.
[5] D.R. Stoll, X. Li, X. Wang, P.W. Carr, S.E.G. Porter, S.C. Rutan, J. Chromatogr. A 1168 (2007) 3.
[6] J.C. Giddings, Anal. Chem. 56 (1984) 1270A.
[7] K. Horie, H. Kimura, T. Ikegami, A. Iwatsuka, N. Saad, O. Fiehn, N. Tanaka, Anal. Chem. (79) (2007) 3764.
[8] L.W. Potts, D.R. Stoll, X. Li, P.W. Carr, J. Chromatogr. A 1217 (2010) 5700.
[9] R.E. Murphy, M.R. Schure, J.P. Foley, Anal. Chem. 79 (1998) 1585.
[10] D.R. Stoll, P.W. Carr, J. Am. Chem. Soc. 127 (2005) 5034.
[11] P. Česla, T. Hájek, P. Jandera, J. Chromatogr. A 1216 (2009) 3443.
[12] A.L. Huidobro, P. Pruim, P.J. Schoenmakers, C. Barbas, J. Chromatogr. A 1190 (2008) 182.
[13] M. Kivilompolo, T. Hyotylainen, J. Sep. Sci. 31 (2008) 3466.
[14] T. Hájek, V. Škeříková, P. Česla, K. Vyňuchalová, P. Jandera, J. Sep. Sci. 31 (2008) 3309.
[15] F. Cacciola, P. Jandera, E. Blahová, L. Mondello, J. Sep. Sci. 29 (2006) 2500.
[16] P. Dugo, F. Cacciola, M. Herrero, P. Donato, L. Mondello, J. Sep. Sci. 31 (2008) 3297.
[17] T. Ikegami, T. Hara, H. Kimura, H. Kobayashi, K. Hosoya, K. Cabrera, N. Tanaka, J. Chromatogr. A 1106 (2006) 112.
[18] P. Jandera, T. Hájek, P. Česla, J. Sep. Sci. 33 (2010) 1362.
[19] F. Cacciola, P. Jandera, Z. Hajdú, P. Česla, L. Mondello, J. Chromatogr. A 1149 (2007) 73.
[20] P. Jandera, J. Churáček, Gradient Elution in Column Liquid Chromatography, Elsevier, Amsterdam, 1985.
[21] L.R. Snyder, J.W. Dolan, High-Performance Gradient Elution. The Practical Application of the Linear-Solvent-Strength Model, Wiley-Interscience, Hoboken, NJ, 2007.
[22] L.R. Snyder, J.W. Dolan, Adv. Chromatogr. 38 (1998) 115.
[23] P. Jandera, J. Chromatogr. A 1126 (2006) 195.
[24] J. Layne, T. Farcas, I. Rustamov, F. Ahmed, J. Chromatogr. A 913 (2001) 233.
[25] M. Czok, A. Katti, G. Guiochon, J. Chromatogr. 550 (1991) 705.
[26] D. Vukmanic, M. Chiba, J. Chromatogr. 483 (1989) 189.
[27] P. Tseng, L.B. Rogers, J. Chromatogr. Sci. 16 (1978) 436.
[28] J. Kirschbaum, S. Perlman, R.B. Poet, J. Chromatogr. Sci. 20 (1982) 336.
[29] F. Khachik, G. Beecher, J. Vanderslice, G. Furrow, Anal. Chem. 60 (1988) 807.
[30] M. Tsimidou, R. Macrae, J. Chromatogr. 285 (1984) 178.
[31] P. Jandera, G. Guiochon, J. Chromatogr. 588 (1991) 1.
[32] C. Castells, R. Castells, J. Chromatogr. A 805 (1998) 55.
[33] M. Mishra, M. Martin, A. De Wit, Chem. Eng. Sci. 65 (7) (2010) 2392.
[34] L. Plante, P. Romano, E. Fernandez, Chem. Eng. Sci. 49 (1) (1994) 2229.
[35] M. Mills, J. Maltas, W. Lough, J. Chromatogr. A 759 (1997) 1.
[36] H. Claessens, M. Kuyken, Chromatographia 23 (1987) 331.
[37] L. Snyder, J. Kirkland, Introduction to Modern Liquid Chromatography, Wiley-Interscience, New York, 1979.
[38] P. Jandera, T. Hájek, J. Sep. Sci. 32 (2009) 3603.
[39] M.A. Quarry, R.L. Grob, L.R. Snyder, Anal. Chem. 58 (1986) 907.
[40] H. Poppe, J. Paanakker, M. Bronkhorst, J. Chromatogr. 204 (1981) 77.
[41] J. Samuelsson, E. Edstrom, P. Forssen, T. Fornstedt, J. Chromatogr. A 1217 (2010) 4306.
[42] G. Guiochon, A. Felinger, D.G. Shirazi, A.M. Katti, Fundamentals of Preparative and Nonlinear Chromatography, 2nd ed., Academic Press, Boston, MA, 2006.
[43] J. Stahlberg, J. Chromatogr. A 1217 (2010) 3172.